SKELETON BASED HOOK ECHO DETECTION IN RADAR REFLECTIVITY DATA

Hongkai Wang, John L. Barron, Robert E. Mercer
{**barron,mercer**}**@csd.uwo.ca**
Dept. of Computer Science
University of Western Ontario
London, Ontario, Canada, N6A 5B7

Paul Joe
Paul.Joe@ec.gc.ca
King City Radar Station
Meteorological Service of Canada
Toronto, Ontario, Canada, M3H 5T4

Abstract: Automatic detection of severe weather events is of great interest to meteorologists. In this paper, we describe and evaluate a method to identify hook echoes automatically in radar reflectivity data. The method is based on the skeletonization of 2D shapes which are used to describe the shape of storms. We use 4 skeleton shape features: curvature, curve orientation, thickness variation and boundary proximity, and two shape features of the 2D object: southwest localization and size to detect hook echoes. We use these features to design a hook echo algorithm. We evaluate this algorithm on hook echoes detected in several radar datasets, which are verified against those manually identified by an human expert.

Keywords: Hook Echo Modelling, Tornadoes, Skeletonization, FAR/POD/CSI Analysis.

1 Introduction

This paper describes an automatic hook echo detection algorithm. Figure 1 shows a hook echo that was part of the May 3^{rd}, 1999 Oklahoma severe weather outbreak.

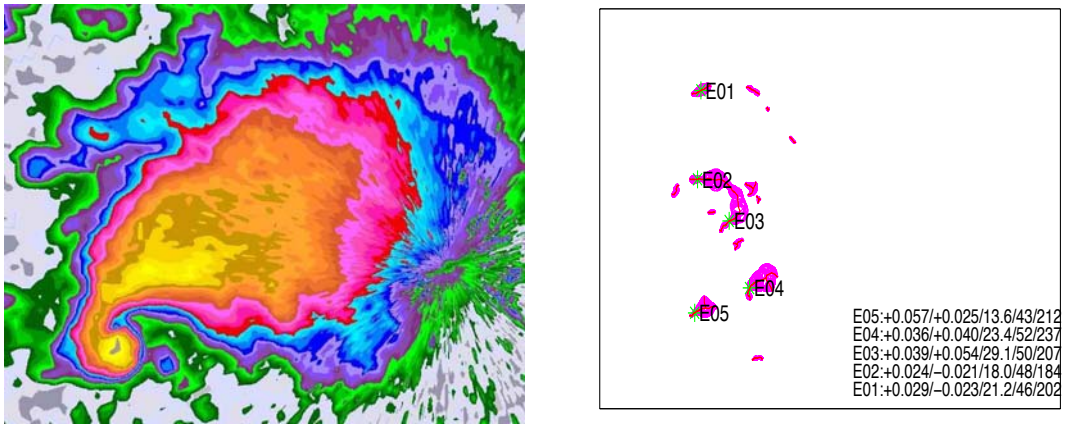

(a) (b)

Figure 1: (a) A classic hook echo (coloured yellow and orange), with the colour table shown on the right hand side and (b) hook echoes detected for the May 3^{rd} 1999, reflectivity data.

Storms are represented as skeletons. A skeleton is an interior contour of a region whose points are the locus of the centers of all maximally inscribed disks. We use the Hierarchic Voronoi Skeleton (HVS) algorithm [OK95] to perform skeletonization because it has a flexible tunable multi-hierarchical capability which is appropriate for finding small scale features (like hooks) embedded in a larger feature (the storm). A skeleton computed by the HVS algorithm for the storm in Figure 1 is shown in Figure 2a.

2 Hook Echo Modelling Methods

The basic idea is to employ skeletons as shape descriptors of storms and then to detect pieces of the storm skeletons that match the properties of the hook echo model. The basics are outlined in the subsections below.

2.1 Image Segmentation

The data set for the lowest elevation in the NEXRADII data is used since the hook echo is expected to be seen only at low levels. The segmentation steps are:

1. Bilinear interpolation is used to "fill-in" the data to have 125m pixel resolution to have smooth images.

2. Binary storm images are computed using the same threshold suggested by Johnson et al. [JMW+98] of 35dBZ on the reflectivity values.

3. Two passes of a 3×3 median filter further eliminates small storms and smooth storm boundaries.

4. Lastly, we eliminate "hole" artifacts in the image data using floodfilling [Wan05, WMBJ07].

2.2 Skeletonization

The parameters of the HVS algorithm are tuned to effectively capture the backbone and the hook-like shapes near the storm boundary. These parameters control the detection and clustering of skeleton branches and are described elsewhere [Wan05, WMBJ07]. Skeletonization converts the 2-D storm into a "backbone" skeleton represented by a (possible bifurcated) polyline.

2.3 Basic Features of the Hook Echo Model

The next task is to detect hooks in the skeleton representation. We extract:

1. **Curvature:** the curvature of the hook portion of the skeleton has a large absolute value. As shown in Figure 2b, along the skeleton branch, the position of the hook (indicated as A) has a relatively high curvature value.

2. **Orientation:** the orientation of the hook correlates strongly to hemispheric rotation: counter-clockwise is dominant in the northern hemisphere and clockwise is dominant in the southern hemisphere. In Figure 2b, the rotating arrow labelled C indicates the orientation of this hook as counter-clockwise (from the inner side to the endpoint). Detecting the orientation of hook echoes can help to rule out false positives.

3. **Thickness Variation:** the hook portion of the skeleton has a distinctive fat-thin-fat (bottle-neck) thickness variation between its surrounding boundary in close proximity to the region of high skeleton curvature. Figure 2c shows the result of straightening the curved skeleton in Figure 2a. This straightening suppresses the curvature property and only the thickness variation along the skeleton is illustrated. In Figure 2d, a hook (its high curvature region is indicated as B) can be seen that exhibits the fat-thin-fat property.

4. **Boundary Proximity:** the hook is near (touching or almost touching) the ends of the protruding parts of the storm shapes. As shown in Figure 2d, if a certain distance threshold value for being near such boundaries is set, for example, in the range M and N marked in the figure, then hook echoes are detected in those ranges. The endpoints of skeletons (boundaries of the topology) approximate the protruding storm boundaries in the hook echo model.

5. **Southwest Localization:** hook echoes tend to exhibit themselves in the southwest quadrant of the main storm region in the northern hemisphere (to the northwest in the southern hemisphere). A direction vector is used to capture this feature in the hook echo model.

6. **Storm Size:** the hook echo is associated with relatively large storms. The length of the skeleton (the maximum arclength distance marked on the skeleton distance map) provides an estimate of the actual storm size.

The actual computations that are used to compute these features are given elsewhere [Wan05, WMBJ07].

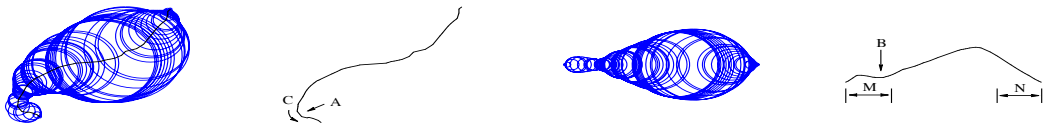

(a) Shape and skeleton (b) Curvature variation (c) Skeleton straightening (d) Thickness variation

Figure 2: (a) The skeleton of an actual storm shape and its disk reconstruction, (b) the curvature variation along the skeleton (A indicates a high curvature location and C indicates the hook's orientation), (c) straightening the skeleton to eliminate its curvature property and only show its thickness variation property and (d) the thickness variation along the skeleton (B indicates the fat-thin-fat location).

3 Experimental Results

The six criteria introduced in the previous section are used to compute the values for the hook echo features. These feature are logically ANDed to detect hooks. That is, to be a hook, it must satisfy every feature criteria, otherwise it is rejected.

In order to evaluate the performance of our detection algorithm, an expert (the last author) independently provided the ground truth for three cases. Following Forbes [For81], definite hook echoes were labelled as 'well-formed' and possible hook echoes were labelled 'marginal'.

The detection results were compared with the ground truth and classify the results into three categories:

- **hits**: correct detection, that is, our detection matches with the estimated ground truth;
- **misses**: false negative, that is, the estimated ground truth indicates it is a hook, while the detection algorithm indicates that it is not;
- **false alarms**: false positive, that is, the estimated groundtruth indicates it is not a hook, while our detection result reports it is.

Note that we cannot count correct negatives.

The experimental results for the radar time of 23:56:21 of dataset `KTLX19990503` are shown in Figure 1b. These two times at a moment when there were well-formed hook echoes.

Hook echo detection results are marked on the skeletons and the relevant numbers are printed in the legends of the figures. For each detected location, its curvature, orientation, thickness variation, boundary proximity, reflectivity and direction angle values are printed in the legend (lower right corner of the image). The format of a legend item is: `Ex: y/z/m/n/p` where `x` is the detected hook echo number, `y` is the absolute value of the curvature value, the sign of `y` shows the orientation (+ for counter-clockwise and - for clockwise), `z` is the thickness variation value, `m` is the boundary proximity value, `n` is reflectivity value and `p` is the direction angle value (in degrees).

Detection results have been evaluated statistically using the Critical Success Index. The first score that we compute is the **False Alarm Ratio** (*FAR*). It is the number of false alarms divided

Datasets	Well-formed Hooks Detected (POD score)	Marginal Hooks Detected (POD score)	False Alarms	POD Score	FAR Score	CSI Score
KTLX19990503 whole, 86 frames	102/126=81.0%	72/119=60.5%	270	71.0%	60.8%	33.8%
KTLX19990503 1^{st} half, 43 frames	57/66=86.4%	30/46=65.2%	68	77.7%	43.9%	48.3%
KTLX19990503 2^{nd} half, 43 frames	45/60=75.0%	42/73=57.5%	202	65.4%	69.9%	26.0%

Table 1: CSI analysis for a radar dataset using our Hook Echo detection algorithm.

by the number of total positive forecasts. The second score is the **Probability of Detection** (*POD*). It is the number of hits divided by the number of total observed 'yes' events. The third score is the **Threat Score** (*TS*) or the **Critical Success Index** (*CSI*). It is the numbers of hits divided by the number of hits, misses and false alarms. This score used to balance *POD* and *FAR* scores, and provides a measure of overall skill for verification purpose.

The experimental results for one datasets is shown in Table 1. These results show that our algorithm has considerable skill for well-formed hook echoes. For marginal hooks, the detection ratio is lower, but still show good skill, than that of well-formed hooks.

The KTLX19990503 dataset was split in half and analyzed separately. As shown in the 2^{nd} and 3^{rd} rows in Table 1, such differences exist even in the same dataset. The algorithm works better with well separated individual storms rather than with embedded storms.

4 Conclusions

In this paper, an automatic method to detect hook echoes is presented. This is the first report of such an algorithm. The output of the hook echo algorithm should not be used in isolation but combined with the other algorithm outputs to provide additional reliability in the storm rankings. The experimental results successfully demonstrate that this technique is effective for the hook echo detection task.

Future work includes using supervised learning techniques to tune the algorithm automatically to improve detection performance.

References

[For81] G.S. Forbes. On the reliability of hook echoes as tornado indicators. *Monthly Weather Review*, 109:1457–1466, 1981.

[JMW+98] J.T. Johnson, P.L. Mackeen, A. Witt, E.D. Mitchell, G.J. Stumpf, M.D. Eilts, and K. W. Thomas. The storm cell identification and tracking algorithm: an enhanced wsr-88d algorithm. *AMS Weather and Forecasting*, 13(2):263–276, 1998.

[OK95] R.L. Ogniewicz and O. Kuebler. Hierarchic voronoi skeletons. *Pattern Recognition*, 28(3):343–359, 1995.

[Wan05] H. Wang. Skeleton-based hook echo detection in doppler radar precipitation density imagery. Master's thesis, The Dept. of Computer Science, The University of Western Ontario, December 2005.

[WMBJ07] H. Wang, R. E. Mercer, J.L. Barron, and P. Joe. Skeleton-based tornado hook echo detection. In 14^{th} *IEEE Intl. Conf. on Image Processing*, volume VI, pages 361–364, 2007.